# First-principles *GW* calculations of GaAs clusters and crystal using an all-electron mixed basis approach

Erm Kikuchi, Shohei Iwata, Soh Ishii, and Kaoru Ohno
*Department of Physics, Graduate School of Engineering, Yokohama National University, 79-5 Tokiwadai, Hodogaya, Yokohama 240-8501, Japan*

(Received 2 April 2007; revised manuscript received 12 June 2007; published 14 August 2007)

All-electron *GW* calculations beginning with the local density approximation of the density functional theory are carried out for both small gallium arsenide clusters and gallium arsenide crystal in a consistent way by means of the all-electron mixed basis approach, in which both plane waves and atomic orbitals are used as a basis set. This approach has the merit of expressing both core electron states and empty free-electron-like states accurately with a rather small number of basis functions. The present all-electron *GW* method enables us to treat both clusters and crystal without difficulty. First, we determined the most stable structures of gallium arsenide clusters, $Ga_nAs_n$ with $n=2-4$. For these clusters, since the structural change in the ionization process is not so large compared to silicon or germanium clusters, there is no significant difference in the vertical and adiabatic electron affinities. For both clusters and crystal, our one-shot *GW* results for quasiparticle energy spectra agree fairly well with available experimental photoemission and inverse photoemission data. The present results include the semirelativistic effect.

DOI: 10.1103/PhysRevB.76.075325 PACS number(s): 79.60.Bm, 71.15.Ap, 71.15.Qe, 61.46.Bc

## I. INTRODUCTION

Physical properties of clusters and crystals are very different from each other. For example, the bulk has a specific value of the energy gap, while clusters have the energy gap depending on the cluster size. Some small semiconductor clusters undergo structural change under excitation,[1–5] while crystals composed of the same elements do not. For heavy elements, the amount of the band gap of some semiconductor crystals, e.g., Ge and GaAs crystals, is quite sensitive to the relativistic effect.

In theoretical studies, since the eigenvalues obtained by the density functional theory (DFT) do not correspond to the quasiparticle energies except for the highest occupied level,[6] the DFT within the local density approximation (LDA) underestimates the energy gap by about 30%–50%. On the other hand, the quasiparticle approach based on the many-body perturbation theory, which is equivalent to determine the poles of the one-particle Green's function, has the merit of giving the whole quasiparticle energy spectra in a single calculation. In particular, the first-principles *GW* calculation beginning with the LDA of the DFT is known to present reliable quasiparticle energy spectra.[7–9] The "*GW* approximation" (GWA) introduced first by Hedin[7] treats the self-energy term approximately as a product of the one-particle Green's function ($G$) and the dynamically screened Coulomb interaction ($W$) within the random phase approximation (RPA). However, such perturbative methods always need an infinite sum of the empty states and in turn a complete set representation of the electronic states. For clusters, because there are infinite free-electron-like states lying above the vacuum level, these methods cannot be applied in terms of the linear combination of atomic orbital approaches using only a localized basis set, which does not span the whole space of the system. On the other hand, for crystals, plane waves can be a good basis except for core states.

Most of the previous *GW* calculations have been applied to semiconductor crystals and are mainly based on the pseudopotential approach.[8–10] Recently, all-electron *GW* calculations on the basis of the full potential linear-muffin-tin orbital (FP-LMTO) approach[11] and the full potential projector-augmented-wave (FP-PAW) approach[12] have appeared in the course of the investigation of semiconductors. However, these approaches cannot be easily applied to isolated systems such as clusters and molecules. The all-electron mixed basis *GW* approach, which we will use in the present work, can be applied to both isolated and crystalline systems in a consistent way. In this approach, a one-particle wave function is expanded in linear combination of both atomic orbitals (AOs) and plane waves (PWs). We use numerical AOs determined inside the nonoverlapping atomic spheres. The merit of this approach is that one can treat both the core electron states and the empty free-electron-like states accurately. This all-electron mixed basis *GW* approach has been successfully applied to alkali-metal clusters[13,14] as well as silicon[2] and germanium clusters.[4]

In the previous paper of silicon[2] and germanium[4] clusters, which we will refer to as I and II, respectively, we clarified by means of the all-electron mixed basis *GW* calculation that the photoemission and inverse photoemission processes are greatly affected by the change of the structures in the ionization process. In particular, $Si_n$ and $Ge_n$ with $n=5$ and 6 undergo large structural change in the ionization process, resulting in the significant difference between the adiabatic and vertical electron affinities (EAs), although no such difference appears in the ionization potential (IP). This is, however, not the common feature of the other clusters, e.g., alkali-metal clusters,[13,14] where this effect is not important because of the large screening among electrons.

In the present paper, we extend our previous studies I and II to gallium arsenide systems and investigate the quasiparticle energy spectra of gallium arsenide crystal as well as small gallium arsenide clusters ($Ga_nAs_n$, $n=2-4$) by means of the first-principles *GW* calculation using the all-electron mixed basis approach. This study presents calculations for

 

both crystalline and cluster systems simultaneously with an all-electron *GW* method. We compare our results with the available experimental photoemission spectra. For clusters, we discuss the structural change between neutral clusters and anions and examine the common characteristics in the behavior of semiconductor clusters. We have included the semirelativistic effect, i.e., the Darwin and mass-velocity terms in all calculations.

## II. METHODOLOGY

Our formulation of the all-electron GWA is the so-called one-shot *GW* and is essentially based on the original paper by Hybertsen and Louie,[8] who used the pseudopotential approach. We start from the calculation at the LDA level and determine the wave functions $\phi_{nk}$ and the energy eigenvalues $\varepsilon_{nk}^{\mathrm{LDA}}$ to evaluate $G$ and $W$ from the viewpoint of perturbation theory.

In the many-body-perturbation theory, the quasiparticle energies $E_{nk}^{\mathrm{QP}}$ can be obtained by solving the Dyson equation,

$$(T+V_{\mathrm{nuc}}+V_H)\phi_{nk}^{\mathrm{QP}}(\boldsymbol{r})+\int d\boldsymbol{r}'\Sigma(\boldsymbol{r},\boldsymbol{r}';E_{nk}^{\mathrm{QP}})\phi_{nk}^{\mathrm{QP}}(\boldsymbol{r}') = E_{nk}^{\mathrm{QP}}\phi_{nk}^{\mathrm{QP}}(\boldsymbol{r}). \tag{1}$$

Here, $T$, $V_{\mathrm{nuc}}$, $V_H$, and $\Sigma$ are the kinetic energy operator, the nucleus Coulomb potential, the Hartree potential, and the self-energy operator, respectively. Using shorthand notation, $1=(\boldsymbol{r}_1,t_1,\sigma_1)$, etc., the self-energy operator is defined via

$$\Sigma(1,2)=i\int G(1,3)W(4,1^+)\Gamma(3,2,4)d(34), \tag{2}$$

where $G$, $\Gamma$, and $W$ denote the Green's function, the 3-point vertex function, and the dynamically screened Coulomb interaction, respectively. So far, everything is exact. Here, we employ an approximation called *GW* approximation introduced by Hedin,[7] where the self-energy operator is approximated by

$$\Sigma(1,2)=iG(1,2)W(1^+,2), \tag{3}$$

corresponding to $\Gamma=1$. Consequently, $W$ is approximated within the RPA. Although Eq. (1) should be solved self-consistently in principle, we adopt the one-shot *GW* calculation. That is, we use unperturbed Green's function instead of renormalized Green's function for the evaluation of $\Sigma$, because using such approximations that $\Gamma$ is always unity contradicts with the exact relationship, Ward-Takahashi identity (see, for example, Ref. 15).

The dynamically screened Coulomb interaction $W$ is related to the dielectric matrix, which is defined by

$$\varepsilon_{GG'}(\boldsymbol{q},\omega)=\delta_{GG'}-v(\boldsymbol{q}+\boldsymbol{G})P_{GG'}(\boldsymbol{q},\omega), \tag{4}$$

through the relation $W_{GG'}(\boldsymbol{q},\omega)=[\varepsilon_{GG'}(\boldsymbol{q},\omega)]^{-1}v(\boldsymbol{q}+\boldsymbol{G}')$. Here, $\boldsymbol{q}$ is the momentum transfer, $\boldsymbol{G},\boldsymbol{G}'$ are reciprocal lattice vectors, and $v(\boldsymbol{q}+\boldsymbol{G})=4\pi/\Omega|\boldsymbol{q}+\boldsymbol{G}|^2$ is the Coulomb potential in Fourier space ($\Omega$ is the volume of the unit cell). The polarizability function in the RPA is given by

$$P_{GG'}(\boldsymbol{q},\omega=0)=\sum_{nn_1\boldsymbol{k}}\langle n\boldsymbol{k}|e^{-i(\boldsymbol{q}+\boldsymbol{G})\cdot\boldsymbol{r}}|n_1\boldsymbol{k}+\boldsymbol{q}\rangle \times\langle n_1\boldsymbol{k}+\boldsymbol{q}|e^{i(\boldsymbol{q}+\boldsymbol{G}')\cdot\boldsymbol{r}'}|n\boldsymbol{k}\rangle \times\frac{f(\varepsilon_{n_1\boldsymbol{k}+\boldsymbol{q}}^{\mathrm{LDA}})-f(\varepsilon_{n\boldsymbol{k}}^{\mathrm{LDA}})}{\varepsilon_{n_1\boldsymbol{k}+\boldsymbol{q}}^{\mathrm{LDA}}-\varepsilon_{n\boldsymbol{k}}^{\mathrm{LDA}}}, \tag{5}$$

where $f(\varepsilon)$ denotes the Fermi-Dirac distribution function. The matrix elements in the numerator involve the intermediate states $|n_1\boldsymbol{k}+\boldsymbol{q}\rangle$.

The self-energy operator $\Sigma$ can be divided into two parts: one is the Fock exchange part $\Sigma_x(\boldsymbol{r},\boldsymbol{r}')$ and the other is the correlation part $\Sigma_c(\boldsymbol{r},\boldsymbol{r}';E)$. The expectation values of the Fock exchange contribution are given by

$$\Sigma_{x,n\boldsymbol{k}}=\langle n\boldsymbol{k}|\Sigma_x(\boldsymbol{r},\boldsymbol{r}')|n\boldsymbol{k}\rangle =-\sum_{n_1}^{occ}\sum_{\boldsymbol{q}\boldsymbol{G}'}\langle n\boldsymbol{k}|e^{i(\boldsymbol{q}+\boldsymbol{G}')\cdot\boldsymbol{r}}|n_1\boldsymbol{k}-\boldsymbol{q}\rangle \times\langle n_1\boldsymbol{k}-\boldsymbol{q}|e^{-i(\boldsymbol{q}+\boldsymbol{G}')\cdot\boldsymbol{r}'}|n\boldsymbol{k}\rangle v(\boldsymbol{q}+\boldsymbol{G}'), \tag{6}$$

while, for the correlation part of the self-energy, the generalized plasmon-pole model[8] is used to bypass the calculation of the $\omega$ dependence of the dielectric matrices and the $\omega'$ integration required in Eq. (3). Then, the expectation values of the correlation part are given by

$$\begin{aligned}\Sigma_{c,n\boldsymbol{k}}(E)&=\langle n\boldsymbol{k}|\Sigma_c(\boldsymbol{r},\boldsymbol{r}';E)|n\boldsymbol{k}\rangle\\ &=\sum_{n_1}^{occ}\sum_{\boldsymbol{q}\boldsymbol{G}\boldsymbol{G}'}\langle n\boldsymbol{k}|e^{i(\boldsymbol{q}+\boldsymbol{G})\cdot\boldsymbol{r}}|n_1\boldsymbol{k}-\boldsymbol{q}\rangle\\ &\times\langle n_1\boldsymbol{k}-\boldsymbol{q}|e^{-i(\boldsymbol{q}+\boldsymbol{G}')\cdot\boldsymbol{r}'}|n\boldsymbol{k}\rangle\\ &\times\frac{1}{2}\frac{\Omega_{GG'}^2(\boldsymbol{q})}{\tilde{\omega}_{GG'}(\boldsymbol{q})[E-\varepsilon_{n_1\boldsymbol{k}-\boldsymbol{q}}^{\mathrm{LDA}}+\tilde{\omega}_{GG'}(\boldsymbol{q})]}v(\boldsymbol{q}+\boldsymbol{G}')\\ &+\sum_{n_1}^{emp}\sum_{\boldsymbol{q}G\boldsymbol{G}'}\langle n\boldsymbol{k}|e^{i(\boldsymbol{q}+\boldsymbol{G})\cdot\boldsymbol{r}}|n_1\boldsymbol{k}-\boldsymbol{q}\rangle\\ &\times\langle n_1\boldsymbol{k}-\boldsymbol{q}|e^{-i(\boldsymbol{q}+\boldsymbol{G}')\cdot\boldsymbol{r}'}|n\boldsymbol{k}\rangle\\ &\times\frac{1}{2}\frac{\Omega_{GG'}^2(\boldsymbol{q})}{\tilde{\omega}_{GG'}(\boldsymbol{q})[E-\varepsilon_{n_1\boldsymbol{k}-\boldsymbol{q}}^{\mathrm{LDA}}-\tilde{\omega}_{GG'}(\boldsymbol{q})]}v(\boldsymbol{q}+\boldsymbol{G}'),\end{aligned} \tag{7}$$

where $\tilde{\omega}_{GG'}$ and $\Omega_{GG'}^2(\boldsymbol{q})$ are the same functions as those defined in the paper by Hybertsen and Louie[8] and are related to $\varepsilon_{GG}^{-1}(\boldsymbol{q},\omega=0)$ and the Fourier components of the valence electron density. The summations with respect to $n_1$ in Eqs. (6) and (7) run over either occupied or empty states only, according to the symbol *occ* or *emp*.

In the calculation of isolated clusters, we use a large supercell. We treat only the $\Gamma$ point ($\boldsymbol{k}=0$) contribution and do not have to perform $\boldsymbol{k}$- or $\boldsymbol{q}$-point sampling in evaluating Eqs. (5)–(7). Thus, all calculations with respect to $\boldsymbol{k}$ and $\boldsymbol{q}$ are performed on $\boldsymbol{k}=\boldsymbol{q}=0$. We use the spherical cutoff in the

Coulomb interaction at a certain distance that is larger than the cluster size but smaller than half of the supercell size. This excludes the problem of the singularity at $\boldsymbol{q}+\boldsymbol{G}'=0$ in the Coulomb interaction $v(\boldsymbol{q}+\boldsymbol{G}')$ in Eqs. (6) and (7).

In the calculation of a crystal system, the matrix elements in the numerator in Eqs. (5)–(7) involve the intermediate states $|n_1\boldsymbol{k}+\boldsymbol{q}\rangle$ and $|n_1\boldsymbol{k}-\boldsymbol{q}\rangle$; the summation over $\boldsymbol{k}$ in the whole Brillouin zone is performed in evaluating Eq. (5), while the summation over $\boldsymbol{q}$ inside the irreducible zone is performed in evaluating Eqs. (6) and (7). Then, it is needed to take the average of the degenerate complex of the resulting quasiparticle energies (see Appendix B in Ref. 8). Therefore, we evaluate the polarizability function $P_{GG'}(\boldsymbol{q},\omega=0)$ for many different $\boldsymbol{q}$ points inside the irreducible zone. A particular treatment should be needed in the neighborhood of $\boldsymbol{q}=0$ when $\boldsymbol{G}'=0$ (see Appendix B in Ref. 8) because there is a singularity in the zero momentum transfer of the Coulomb interaction appearing in expressions (6) and (7) of the self-energies $\Sigma_x$ and $\Sigma_c$.

Finally, the *GW* quasiparticle energies $E_{n\boldsymbol{k}}^{\mathrm{GWA}}$ are obtained in terms of the first-order perturbation theory as

$$E_{n\boldsymbol{k}}^{\mathrm{GWA}} \approx \varepsilon_{n\boldsymbol{k}}^{\mathrm{LDA}} + \frac{1}{1-[\partial\Sigma(\omega)/\partial\omega]_{\varepsilon_{n\boldsymbol{k}}^{\mathrm{LDA}}}} \times\langle n\boldsymbol{k}|\{\Sigma(\varepsilon_{n\boldsymbol{k}}^{\mathrm{LDA}})-\mu_{\mathrm{xc}}^{\mathrm{LDA}}\}|n\boldsymbol{k}\rangle, \quad (8)$$

where the denominator in the second term is the renormalization factor.

## III. *GW* CALCULATION OF GALLIUM ARSENIDE CLUSTERS

### A. Geometry of gallium arsenide clusters

In photoemission and inverse photoemission processes, structural changes in the photoionization are important. Here, we first determine the most stable structure of neutral and negatively charged gallium arsenide clusters. Although the structure of $Ga_nAs_n$ was studied by other authors,[5,16–22] the most stable structure of $Ga_3As_3$ and $Ga_4As_4$ reported in some papers does not coincide with that of other papers. Therefore, we performed again structural optimizations using the GAUSSIAN03 program package[23] within the LDA. We compare the total energy using the Slater-Vosko-Wilk-Nussair exchange-correlation potential with 6-311+G** basis set and determine the lowest-energy structure of the neutral clusters and anions. Figures 1–3 show the obtained structures. In Table I, we show relative total energies (in eV) of $Ga_nAs_n$ ($n=2-4$) in neutral condition. The most stable structure of $Ga_2As_2$ has $D_{2h}$ symmetry, which is the same as the previous studies.[5,16,17,21] The As-As bond length is 2.28 Å, corresponding to the short diagonal bond (2.62 Å) of $Ge_4$, although the Ga-Ga bond of $Ga_2As_2$, which is 2.62 Å on each side, is longer than that of $Ge_4$, which is 2.48 Å on each side (see II). Structure c of $Ga_3As_3$ is the most stable among three structures, which is found to be 0.29 eV more stable than structure b. The Ga-As bond length (about 2.70–2.79 Å, one is 2.49 Å) is larger than the As-As bond length (2.45 Å). In contrast, the Ga-Ga bond length (2.63 Å) is intermediate between Ga-As and As-As bond lengths. Structure e (Fig. 2) of $Ga_4As_4$ is the most stable. The detailed bond lengths are given in Fig. 3. The As-As bond length of e (Fig. 3) is 2.43 Å, similar to that of $Ga_3As_3$. In contrast, the adjacent Ga-As and Ga-Ga bond lengths are, respectively, about 2.37–3.17 and 2.53–3.05 Å. $Ga_4As_4$ has $C_i$ symmetry in accordance with the paper by Piquini *et al.*[5] For $Ga_2As_2$, the change in the bond lengths between neutral and negatively charged clusters is at most 0.14 Å, which is similar to $Si_4$ and $Ge_4$ reported in I and II. For $Ga_3As_3$, the change in the bond lengths is further small and at most 0.11 Å, which is much smaller than that of $Si_5$, $Si_6$, $Ge_5$, and $Ge_6$ reported in I and II. Concerning $Ga_4As_4$, because the distance of the short bonds is not affected much due to the strong interaction of the tetrahedral covalent bonds, the overall structural change between the anion e′ and neutral e clusters (Fig. 3) is not so large. This structural change affects little the exchange-correlation energy, as will be discussed in Sec. III C.

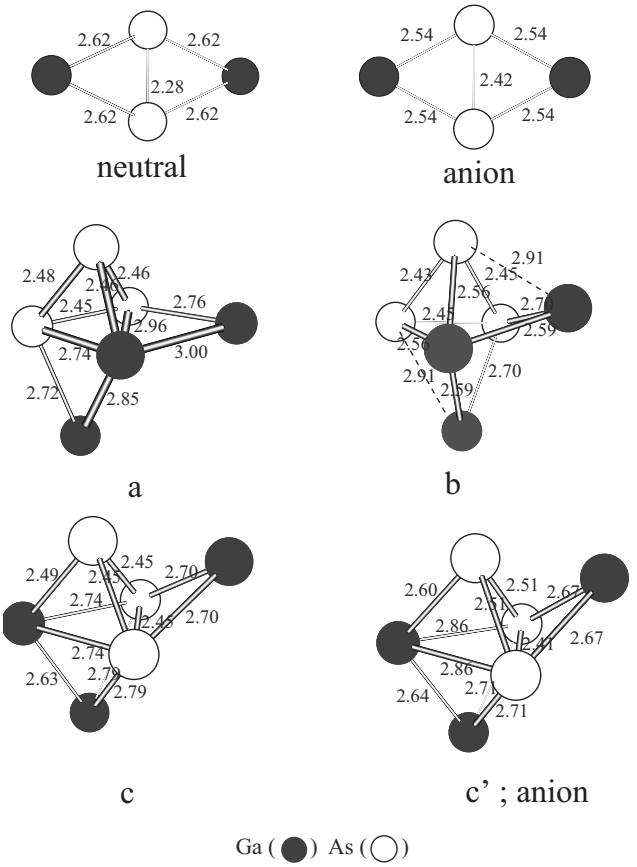


FIG. 1. The geometry of $Ga_nAs_n$ and $Ga_nAs_n^-$ ($n=2,3$). Ga atoms are represented by dark spheres and As atoms by white spheres. These structures previously determined in Refs. 17, 20, and 22 were newly optimized with the LDA. The numbers indicate the bond lengths in Å. a is the same structure as given in Refs. 17 and 22, but the others are all newly optimized in the present study. b is the optimized structure using structure a. c is the structure as given in Refs. 17, 20, and 22. c′ is negatively charged structure using structure c.

In Table II, we show relative total energies (in eV) of $Ga_nAs_n$, $Ga_nAs_n^{(-)-}$, and $Ga_nAs_n^{(0)-}$ ($n=2-4$). $Ga_nAs_n^{(-)}$ and

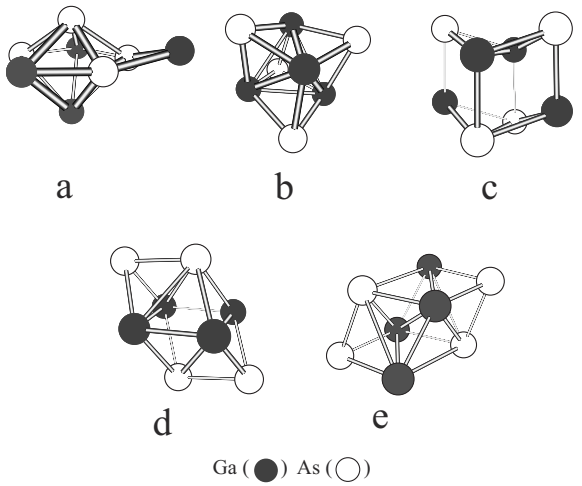


FIG. 2. The geometry of $Ga_4As_4$ isomers. Ga atoms are represented by dark spheres and As atoms by white spheres. These structures previously determined in Refs. 17–19, 21, and 22 were newly optimized with the LDA. (a) Reference 18, (b) Refs. 18 and 19, (c) Ref. 17, (d) Refs. 19 and 21, and (e) Refs. 18, 21, and 22.

$Ga_nAs_n^{(0)}$ denote the most stable structure of anion and neutral clusters (see Figs. 1 and 3), and the right side figures "−" and "0" in their superscript denote negatively charged and neutral electronic states.

### B. *GW* calculation

In the *GW* calculation of gallium arsenide clusters, we use the lowest-energy structure in each size of the clusters. We adopt an fcc supercell with a cubic edge of 18 Å. We use 18 numerical AOs ($1s$, $2s$, $2p\times3$, $3s$, $3p\times3$, $3d\times5$, $4s$, $4p\times3$) for each atom and 8099 PWs corresponding to the cutoff energy of 6.7 Ry. For the evaluation of $P_{GG'}(\boldsymbol{q},\omega=0)$ and $\Sigma_{\mathbf{c},n\boldsymbol{k}}$, 3000 states are used in the summation over $n$ (and $n_1$) in Eqs. (5) and (7), and 2975 $\boldsymbol{G}(\boldsymbol{G}')$ corresponding to the cutoff energy of 3.4 Ry are used. On the other hand, in the calculation of $\Sigma_{x,n\boldsymbol{k}}$, 219 363 $\boldsymbol{G}$ corresponding to the cutoff energy of 60 Ry are used to take into account correctly the core contribution.

TABLE I. Relative total energies (in eV) of $Ga_nAs_n$ ($n=2-4$).

| | | Point group | State | Relative energy |
|---|---|---|---|---|
| $Ga_2As_2$ | | $D_{2h}$ | $^1A_g$ | |
| | Fig. 1 | Point group | state | Relative energy |
| $Ga_3As_3$ | a | $C_1$ | $^1A$ | 0.79 |
| $Ga_3As_3$ | b | $C_1$ | $^1A$ | 0.29 |
| $Ga_3As_3$ | c | $C_S$ | $^1A$ | 0.00 |
| | Figs. 2 and 3 | Point group | State | Relative energy |
| $Ga_4As_4$ | a | $C_1$ | $^1A$ | 1.05 |
| $Ga_4As_4$ | b | $C_3$ | $^1A$ | 0.61 |
| $Ga_4As_4$ | c | $C_{2v}$ | $^1A$ | 0.38 |
| $Ga_4As_4$ | d | $C_{2h}$ | $^1A$ | 0.36 |
| $Ga_4As_4$ | e | $C_i$ | $^1A_g$ | 0.00 |

### C. Results and discussion

In Table III, the *GW* quasiparticle energies (GWQPEs) $E_n^{\mathrm{GWA}}$ are listed together with the LDA energy eigenvalues $\varepsilon_n^{\mathrm{LDA}}$ and the experimental IPs[24] and EAs[25] with minus signs, $E_n^{\mathrm{expt}}$. In the first column, $Ga_nAs_n$ with $n=2-4$ denote neutral clusters with the most stable ground-state geometry, while $Ga_nAs_n^{(-)0}$ with $n=2-4$ denote neutral clusters with the optimized geometry of anions. The former corresponds to the vertical transition, and the latter corresponds to the adiabatic transition for EA [the absolute lowest-unoccupied (LUMO) energy is EA]. For the highest occupied molecular orbital (HOMO) level of each cluster, the LDA eigenvalue is far off the resulting GWQPE in spite of the exact theorem.[6] Once again, the absolute HOMO energy is IP.[6] This indicates that the LDA is not an accurate approximation within the DFT.

In the same table, we also show the other contributions to the GWQPEs [see Eq. (8)], i.e., the expectation values of the LDA exchange-correlation potential $\mu_{\mathrm{xc}}^{\mathrm{LDA}}$, the exchange part $\Sigma_x$, and the correlation part $\Sigma_c$ of the self-energy. Although $\Sigma_{x,n}$ almost does not depend on the cluster size for the HOMO level, it depends on the cluster size for the LUMO level. The absolute value of $\Sigma_{x,n}$ for the LUMO level of

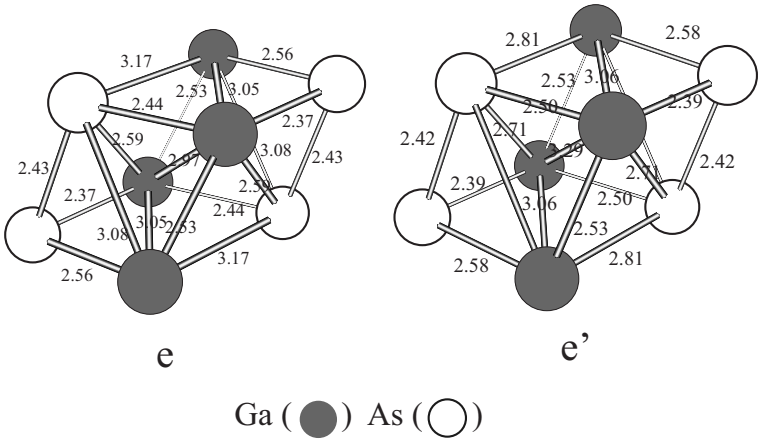


FIG. 3. The geometry of the most stable $Ga_4As_4$ isomer. Ga atoms are represented by dark spheres and As atoms by white spheres. These structures previously determined in Refs. 18, 21, and 22 were newly optimized with the LDA. The numbers indicate the bond lengths in Å. e (Ref. 18) is neutral and e′ (Refs. 21 and 22) is anion.

TABLE II. Relative total energies (in eV) of the anion and neutral clusters for $Ga_nAs_n$ ($n$=2–4). $Ga_nAs_n^{(0)-}$ and $Ga_nAs_n^{(-)-}$ are anions calculated for geometries of neutral and negatively charged clusters, respectively.

| | | Point group | State | Relative energy |
|---|---|---|---|---|
| $Ga_2As_2$ | | $D_{2h}$ | $^1A_g$ | 2.31 |
| $Ga_2As_2^{(0)-}$ | | $D_{2h}$ | $^2B_{1g}$ | 0.22 |
| $Ga_2As_2^{(-)-}$ | | $D_{2h}$ | $^2B_{1g}$ | 0.00 |
| | Fig. 1 | Point group | State | Relative energy |
| $Ga_3As_3$ | c | $C_S$ | $^1A$ | 1.80 |
| $Ga_3As_3^{(0)-}$ | c | $C_S$ | $^2A'$ | 0.13 |
| $Ga_3As_3^{(-)-}$ | c′ | $C_S$ | $^2A'$ | 0.00 |
| | Figs. 2 and 3 | Point group | State | Relative energy |
| $Ga_4As_4$ | e | $C_i$ | $^1A_g$ | 2.43 |
| $Ga_4As_4^{(0)-}$ | e | $C_i$ | $^2A_u$ | 0.06 |
| $Ga_4As_4^{(-)-}$ | e′ | $C_i$ | $^2A_u$ | 0.00 |

$Ga_3As_3^{(-)0}$ is 1.0 eV, which is 1.7 eV less than that of $Ga_2As_2^{(-)0}$ and $Ga_4As_4^{(-)0}$. However, these contributions tend to be compensated by the negative contribution from $\mu_{xc,n}^{LDA}$, and therefore the final results for the GWQPEs are not affected so much. If we compare the results of $Ga_nAs_n$ and $Ga_nAs_n^{(-)0}$ with same $n$, each contribution ($\mu_{xc,n}^{LDA}$, $\Sigma_{c,n}$, and $\Sigma_{x,n}$) to the correction to the LDA eigenvalues has similar values, reflecting the insensitiveness of each contribution to the structural difference between neutral and negatively charged clusters. Hence, the difference in the LDA eigenvalues between $Ga_nAs_n$ and $Ga_nAs_n^{(-)0}$ seems to reflect directly the difference in the resulting GWQPEs. The obtained HOMO-LUMO gap monotonically decreases with cluster size. This tendency is not seen in other semiconductor clusters such as silicon and germanium, in which the HOMO-LUMO gap does not strongly depend on the cluster size as seen in I and II. This tendency is somewhat similar to the metallic clusters.[13,14]

When we compare our results with experimental data, we first note that the experimental IPs of $Ga_nAs_n$ are such that 6.4 eV$<$IP$\leqslant$7.9 eV.[24] The data are available only for $Ga_nAs_n$ with odd $n$. The resulting GWQPEs for the HOMO level of each cluster are all consistent with this experiment. Our results for the vertical (adiabatic) EAs of dimer, trimer, and tetramer estimated from the GWQPEs are 1.90 (2.13), 1.71 (1.84), and 2.50 (2.66) eV, respectively (see also Fig. 4). Jin *et al.*[25] measured the photodetachment thresholds and reported that they estimated vertical EAs. Anyway, as is seen in Fig. 4, the difference between the vertical and adiabatic EAs in $Ga_nAs_n$ is small and less than 0.2 eV, although that of $Ge_5$ and $Ge_6$ reported in II is large, about 0.8 and 0.65 eV. In

TABLE III. The comparison (in eV) of the GWQPEs ($E_n^{GWA}$) for the HOMO and LUMO levels of gallium arsenide clusters with the LDA eigenvalues ($\varepsilon_n^{LDA}$) and the experimental electron affinities (Ref. 25) with minus signs ($E_n^{expt}$). HOMO and LUMO correspond, respectively, to IP and EA. An available experimental ionization potential of $Ga_nAs_n$ is such that 6.4 eV$<$IP$\leqslant$7.9 eV (Ref. 24), whose higher bound is shown inside the parentheses. The final result $E_n^{GWA}$ is evaluated through Eq. (8): $\mu_{xc,n}^{LDA}=\langle n|\mu_{xc}^{LDA}|n\rangle$, $\Sigma_{x,n}=\langle n|\Sigma_x|n\rangle$, and $\Sigma_{c,n}=\langle n|\Sigma_c|n\rangle$ are the expectation values of, respectively, the LDA exchange-correlation potential and the exchange and correlation parts of the self-energy $\Sigma$. In the first column, $Ga_nAs_n$ and $Ga_nAs_n^{(-)0}$ denote neutral clusters with the geometry optimized under neutral and negatively charged conditions, respectively. The former corresponds to the vertical transition, and the latter corresponds to the adiabatic transition for EA.

| | | $\varepsilon_n^{LDA}$ | $\mu_{xc,n}^{LDA}$ | $\Sigma_{x,n}$ | $\Sigma_{c,n}(\varepsilon_n^{LDA})$ | $E_n^{GWA}$ | $E_n^{expt}$ |
|---|---|---|---|---|---|---|---|
| $Ga_2As_2$ | HOMO | −5.27 | −12.03 | −14.26 | −0.79 | −7.99 | (−7.90[a]) |
| | LUMO | −3.90 | −11.62 | −7.73 | −1.67 | −1.90 | −2.10±0.10[b] |
| $Ga_2As_2^{(-)0}$ | HOMO | −4.92 | −11.95 | −14.18 | −0.78 | −7.65 | (−7.90[a]) |
| | LUMO | −4.39 | −11.76 | −7.90 | −1.60 | −2.13 | −2.10±0.10[b] |
| $Ga_3As_3$ | HOMO | −5.34 | −12.17 | −14.14 | −0.53 | −7.61 | (−7.90[a]) |
| | LUMO | −3.23 | −10.20 | −6.66 | −1.87 | −1.71 | −2.10±0.10[b] |
| $Ga_3As_3^{(-)0}$ | HOMO | −5.32 | −12.15 | −14.13 | −0.51 | −7.59 | (−7.90[a]) |
| | LUMO | −3.46 | −10.49 | −6.93 | −1.81 | −1.84 | −2.10±0.10[b] |
| $Ga_4As_4$ | HOMO | −5.28 | −12.29 | −14.04 | −0.81 | −7.57 | (−7.90[a]) |
| | LUMO | −3.87 | −11.76 | −8.59 | −1.65 | −2.50 | −2.30±0.10[b] |
| $Ga_4As_4^{(-)0}$ | HOMO | −5.08 | −12.19 | −13.81 | −0.91 | −7.34 | (−7.90[a]) |
| | LUMO | −4.26 | −11.74 | −8.59 | −1.62 | −2.66 | −2.30±0.10[b] |

[a]Reference 24.
[b]Reference 25.

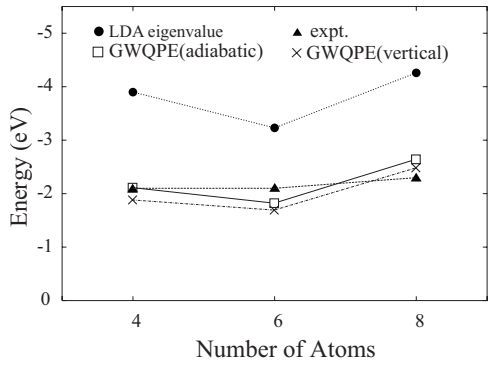


FIG. 4. The cluster-size dependence of the LUMO quasiparticle energy (EA with minus sign) of $Ga_nAs_n$ ($n=2-4$) obtained from the present *GW* calculations (squares and crosses), compared with the LDA eigenvalues (solid circles) and the experimental electron affinities (solid triangles). Both the GWQPEs corresponding to the adiabatic and vertical EAs are shown, respectively, by squares and crosses.

the negatively charged and neutral clusters of $Ga_nAs_n$ ($n=2-4$), the structural change is not so large. This is the reason that the difference between the vertical and adiabatic EAs in $Ga_nAs_n$ is smaller than that in $Ge_n$.

## IV. *GW* CALCULATION OF GALLIUM ARSENIDE CRYSTAL

### A. Calculation

GaAs crystal has a cubic zinc sulfide structure. In the present calculation, we assume the smallest fcc unit cell of the edge length of 3.99 Å inside which a pair of Ga and As atoms is located. The volume of the irreducible zone is 1/24 of the whole Brillouin zone. Since GaAs does not have an inversion symmetry in space, it has the irreducible zone that is composed of a pair of symmetrical wedges about the Γ point. Within the irreducible zone, several symmetrical points (indicated by Γ, *X*, *L*, *K*, *U*, *W*, etc.) exist. For the LDA level calculation, we use four special $\boldsymbol{k}$ points to get convergence of electronic states. In $4\times4\times4$ partition of the whole Brillouin zone, 32 $\boldsymbol{k}$ points including Γ point are used for $P_{\boldsymbol{GG'}}(\boldsymbol{q},\omega=0)$. To evaluate $\Sigma_{x,n\boldsymbol{k}}$ and $\Sigma_{c,n\boldsymbol{k}}(\varepsilon_{n\boldsymbol{k}}^{\mathrm{LDA}})$, the $\boldsymbol{q}$ point sampling is performed inside the irreducible zone including the Γ point. In $6\times6\times6$ partition of the irreducible Brillouin zone, 25 $\boldsymbol{q}$ points inside the irreducible zone are used as the sampling points.

We use 36 numerical AOs and 181 PWs corresponding to the cutoff energy of 11 Ry. For the evaluation of $P_{\boldsymbol{GG'}}(\boldsymbol{q},\omega=0)$ and $\Sigma_{\mathbf{c},n\boldsymbol{k}}$, 120 states are used in the summation over $n$ (and $n_1$) in Eqs. (5) and (7), and 181 $\boldsymbol{G}(\boldsymbol{G'})$ corresponding to the cutoff energy of 11 Ry are used. On the other hand, in the calculation of $\Sigma_{x,n\boldsymbol{k}}$, 17 261 $\boldsymbol{G}$ corresponding to the cutoff energy of 225 Ry are used to take into account correctly the core contribution.

### B. Results and discussion

In Table IV, the GWQPEs $E_{n\boldsymbol{k}}^{\mathrm{GWA}}$ are listed compared to the LDA energy eigenvalues $\varepsilon_{n\boldsymbol{k}}^{\mathrm{LDA}}$ for several valence levels at the Γ, *X*, and *L* points of gallium arsenide crystal. In the same table, we also show the contributions to the GWQPEs, i.e., the expectation values of, respectively, the LDA exchange-correlation part $\mu_{\mathrm{xc},n\boldsymbol{k}}^{\mathrm{LDA}}$, the exchange part $\Sigma_{x,n\boldsymbol{k}}$, and the correlation part $\Sigma_{c,n\boldsymbol{k}}$ of the self-energy. There is no

TABLE IV. The LDA eigenvalues $\varepsilon_{n\boldsymbol{k}}^{\mathrm{LDA}}$ and the GWQPEs $E_{n\boldsymbol{k}}^{\mathrm{GWA}}$, including the semirelativistic effect, estimated at the levels in the vicinity of the band gap of gallium arsenide crystal (in eV). Contributions to the quasiparticle energies are also shown: $\mu_{xc,n\boldsymbol{k}}^{\mathrm{LDA}}=\langle n\boldsymbol{k}|\mu_{xc}^{\mathrm{LDA}}|n\boldsymbol{k}\rangle$, $\Sigma_{\mathrm{x},n\boldsymbol{k}}=\langle n\boldsymbol{k}|\Sigma_{\mathrm{x}}|n\boldsymbol{k}\rangle$, and $\Sigma_{\mathrm{c},n\boldsymbol{k}}=\langle n\boldsymbol{k}|\Sigma_{\mathrm{c}}|n\boldsymbol{k}\rangle$ are the expectation values of, respectively, the LDA exchange-correlation potential and the exchange and correlation parts of the self-energy Σ. There is no meaning in the absolute values of $\varepsilon_{n\boldsymbol{k}}^{\mathrm{LDA}}$ and $E_{n\boldsymbol{k}}^{\mathrm{GWA}}$.

| GaAs | $\varepsilon_{n\boldsymbol{k}}^{\mathrm{LDA}}$ | $\mu_{xc,n\boldsymbol{k}}^{\mathrm{LDA}}$ | $\Sigma_{\mathrm{x},n\boldsymbol{k}}$ | $\Sigma_{\mathrm{c},n\boldsymbol{k}}(\varepsilon_{n\boldsymbol{k}}^{\mathrm{LDA}})$ | $E_{n\boldsymbol{k}}^{\mathrm{GWA}}$ |
|---|---|---|---|---|---|
| $\Gamma_{1v}$ | −4.70 | −14.64 | −18.68 | 5.12 | −3.92 |
| $\Gamma_{15v}$ | 7.76 | −15.80 | −14.30 | 0.04 | 9.06 |
| $\Gamma_{1c}$ | 7.98 | −16.36 | −11.53 | −2.07 | 10.31 |
| $\Gamma_{15c}$ | 11.66 | −12.87 | −7.80 | −3.08 | 13.33 |
| $X_{1v}$ | −2.53 | −16.98 | −19.89 | 4.06 | −1.69 |
| $X_{3v}$ | 1.33 | −13.65 | −15.03 | 2.28 | 2.04 |
| $X_{5v}$ | 5.34 | −13.73 | −13.40 | 0.80 | 6.28 |
| $X_{1c}$ | 9.81 | −10.90 | −6.60 | −2.72 | 11.16 |
| $X_{3c}$ | 10.06 | −12.38 | −7.88 | −2.65 | 11.63 |
| $L_{2v}$ | −3.12 | −16.53 | −19.87 | 4.36 | −2.40 |
| $L_{1v}$ | 1.52 | −13.12 | −14.49 | 2.21 | 2.19 |
| $L_{3v}$ | 6.79 | −14.89 | −13.87 | 0.33 | 7.93 |
| $L_{1c}$ | 8.91 | −14.04 | −9.45 | −2.34 | 10.81 |
| $L_{3c}$ | 12.89 | −12.63 | −7.30 | −3.35 | 14.54 |

TABLE V. LDA eigenvalues $\varepsilon_{n\boldsymbol{k}}^{\mathrm{LDA}}$ at symmetry points of gallium arsenide crystal in eV. The values are measured from the top of the valence band ($\Gamma_{15v}$). The symbols, GTO, PAW, and Present denote Gaussian-type orbital method (Ref. 10), the projector-augmented-wave approach (Ref. 26), and the present all-electron mixed basis approach, respectively.

| GaAs | GTO[a] | PAW[b] | Present |
|---|---|---|---|
| $\Gamma_{1v}$ | −12.69 | −12.79 | −12.46 |
| $\Gamma_{15v}$ | 0.00 | 0.00 | 0.00 |
| $\Gamma_{1c}$ | 0.57 | 0.31 | 0.22 |
| $\Gamma_{15c}$ | 3.75 | 3.65 | 3.90 |
| $X_{1v}$ | −10.37 | −10.28 | −10.29 |
| $X_{3v}$ | −6.79 | | −6.43 |
| $X_{5v}$ | −2.56 | −2.72 | −2.42 |
| $X_{1c}$ | 1.80 | 1.33 | 2.05 |
| $X_{3c}$ | 1.85 | 1.54 | 2.30 |
| $L_{2v}$ | −11.08 | −11.02 | −10.88 |
| $L_{1v}$ | −6.59 | −6.72 | −6.24 |
| $L_{3v}$ | −1.10 | −1.16 | −0.97 |
| $L_{1c}$ | 1.13 | 0.84 | 1.15 |
| $L_{3c}$ | 4.67 | 4.57 | 5.13 |

[a]Reference 10.
[b]Reference 26.

meaning in the absolute values of $E_{n\boldsymbol{k}}^{\mathrm{GWA}}$ as well as $\varepsilon_{n\boldsymbol{k}}^{\mathrm{LDA}}$ because an ambiguity exists in the value of zero energy. As for the level symbols, $\Gamma_{15v}$ is the valence-band top. The conduction-band bottom is $\Gamma_{1c}$. Again, the sum of $\Sigma_{x,n\boldsymbol{k}}$ and $\Sigma_{c,n\boldsymbol{k}}$ has a tendency to compensate the negative contribution from $\mu_{\mathrm{xc},n\boldsymbol{k}}^{\mathrm{LDA}}$ but the compensation is not compete, resulting in the *GW* correction.

Table V lists the LDA energy eigenvalues measured from the top of the valence band ($\Gamma_{15v}$). In this table, we compare the present LDA energy eigenvalues with the previous LDA of the Gaussian-type orbital (GTO)[10] method and the projector-augmented-wave (PAW)[26] method at the symmetry points $\Gamma$, $X$, and $L$. There is visible difference in the LDA eigenvalues of the GTO, PAW, and present approaches. In the case of bulk gallium arsenide, it is well known that, in the LDA level calculation, the semirelativistic effect dramatically reduces the value of the energy gap and only the GWA with the semirelativistic effect reproduces very well the experimental energy gap.[8] In fact, the direct energy gap ($\Gamma_{15v} \rightarrow \Gamma_{1c}$) within the LDA reduces 1.04 eV$\rightarrow$0.22 eV and the GWA with the semirelativistic effect agrees well with experiments.

In Table VI, we compare the results of the present and previous *GW* calculations as well as the experimental data. For each symmetry point, the values of GWQPEs and experiments (Expt.) are listed. The symbols GTO, PAW, FP-PAW, and FP-LMTO denote respectively, the previous theoretical results using the pseudopotential Gaussian-type

TABLE VI. Quasiparticle energies at symmetry points of gallium arsenide crystal in eV. For each symmetry point, the values of GWA results and experiments (Expt.) (Refs. 27 and 28) are listed. The symbols, GTO, PAW, FP-PAW, and FP-LMTO denote, respectively, the previous theoretical results using the pseudopotential Gaussian-type orbital approach (Ref. 10), the projector-augmented-wave approach (Ref. 26), the all-electron full-potential PAW (Ref. 12), and the full-potential linear muffin-tin-orbital approach (Ref. 11). "Present" denotes our all-electron mixed basis approach.

| GaAs | GTO[a] | PAW[b] | FP-PAW[c] | FP-LMTO[d] | Present | Expt.[e] |
|---|---|---|---|---|---|---|
| $\Gamma_{1v}$ | −12.69 | −12.64 | | | −12.98 | −13.21 |
| $\Gamma_{15v}$ | 0.00 | 0.00 | 0.00 | 0.00 | 0.00 | 0.00 |
| $\Gamma_{1c}$ | 1.32 | 1.26 | 1.09 | 1.30 | 1.25 | 1.52 |
| $\Gamma_{15c}$ | 4.60 | 4.19 | | 4.31 | 4.27 | 4.61 |
| $X_{1v}$ | −10.27 | −10.26 | | | −10.75 | −10.86 |
| $X_{3v}$ | −7.16 | | | | −7.02 | −6.81 |
| $X_{5v}$ | −2.71 | −2.77 | | | −2.78 | −2.91 |
| $X_{1c}$ | 2.65 | 1.72 | 1.64 | 1.65 | 2.10 | 1.90 |
| $X_{3c}$ | 2.72 | 2.02 | | 1.99 | 2.57 | 2.47 |
| $L_{2v}$ | −11.02 | −11.04 | | | −11.47 | −11.35 |
| $L_{1v}$ | −6.91 | −6.67 | | | −6.87 | −6.81 |
| $L_{3v}$ | −1.17 | −1.19 | | | −1.14 | −1.41 |
| $L_{1c}$ | 1.92 | 1.53 | 1.53 | 1.55 | 1.75 | 1.74 |
| $L_{3c}$ | 5.65 | 5.04 | | | 5.48 | 5.45 |

[a]Reference 10
[b]Reference 26
[c]Reference 12
[d]Reference 11
[e]References 27 and 28

orbital approach, the pseudopotential projector-augmented-wave approach corrected by the all-electron wave functions,[26] the full-potential PAW approach,[12] and the full-potential linear muffin-tin-orbital approach.[11] All these calculations are one-shot GWA.

In the results of the present calculations, the energy gaps between the valence-band top ($\Gamma_{15v}$) and all levels of each symmetry point agree quite well with the experiments. The difference between the present result and the experimental value is largest (0.34 eV) at $\Gamma_{15c}$, and second largest (0.27 eV) at $\Gamma_{1c}$ (conduction-band bottom) and $L_{3v}$. The average difference is 0.16 eV. The relatively large difference from the experimental values at $\Gamma_{15c}$, $\Gamma_{1c}$, and $L_{3v}$, i.e., the underestimation of the absolute values by about 0.3 eV, is, however, a common characteristic in all other calculations except for the pseudopotential GTO result at $\Gamma_{15c}$,[10] which is in good agreement with the experimental value. The present GWQPEs (as well as the LDA eigenvalues shown in Table V) obtained at $X$ and $L$ points for the conduction bands slightly overestimate experimental values. This behavior is similar to the results of the GTO approach[10] (the second column). This similarity is perhaps due to the use of atomic orbitals in the calculation. On the whole, our all-electron calculation seems to correspond to experiments most accurately of all these calculations, which suggests the validity of the present method within the one-shot *GW*.

## V. CONCLUSION

In summary, we have carried out all-electron *GW* calculations of both small gallium arsenide clusters and gallium arsenide crystal by means of the all-electron mixed basis approach. This approach has the merit of expressing both core electron states and empty free-electron-like states accurately with a rather small number of basis functions. This is particularly useful because it is inevitable to introduce an extended basis set such as plane waves to express free-electron-like states above the vacuum level in the summation over all empty states in the perturbative calculations using the Green's function approach. The present all-electron *GW* method enables one to treat both clusters and crystal in a consistent way without any difficulty. For gallium arsenide clusters, since the structural change in the ionization process is not so large compared to silicon or germanium clusters reported previously in I and II, there is no significant difference in the vertical and adiabatic photoemission spectra. The resulting GWQPEs are, thus, in fairly good agreement with available experimental data for IPs and EAs. Using $\boldsymbol{k}$-point and $\boldsymbol{q}$-point samplings for the calculation of the polarization function $P_{GG'}$ and the self-energy operator $\Sigma$ ($\Sigma_c$ and $\Sigma_c$), we have performed an all-electron *GW* calculation for bulk gallium arsenide crystal and showed the GWQPEs for several levels close to the energy band gap. The results of GWQPEs at several symmetry points are in excellent agreement with the experimental photoemission data. Thus, the present one-shot *GW* calculation using the all-electron mixed basis approach beginning with the LDA of the DFT is found to be quite good for both clusters and crystals.

## ACKNOWLEDGMENTS

The authors thank the Hokkaido University Information Initiative Center for the support of the SR11000 supercomputing facilities. This work has been partly supported by the Grant-in-Aid for Scientific Research B (No. 17310067) and Scientific Research on Priority Area (No. 18036005) from the Japan Society for the Promotion of Science and from the Ministry of Education, Culture, Sports, Science and Technology of Japan.

[1] N. Binggeli and J. R. Chelikowsky, Phys. Rev. Lett. **75**, 493 (1995).
[2] S. Ishii, K. Ohno, V. Kumar, and Y. Kawazoe, Phys. Rev. B **68**, 195412 (2003).
[3] E. F. Archibong and A. St-Amant, J. Chem. Phys. **109**, 962 (1998).
[4] E. Kikuchi, S. Ishii, and K. Ohno, Phys. Rev. B **74**, 195410 (2006).
[5] P. Piquini, S. Canuto, and A. Fazzio, Nanostruct. Mater. **10**, 635 (1998).
[6] C.-O. Almbladh and U. von Barth, Phys. Rev. B **31**, 3231 (1985).
[7] L. Hedin, Phys. Rev. **139**, A796 (1965).
[8] M. S. Hybertsen and S. G. Louie, Phys. Rev. Lett. **55**, 1418 (1985); Phys. Rev. B **34**, 5390 (1986).
[9] R. W. Godby, M. Schlüter, and L. J. Sham, Phys. Rev. B **37**, 10159 (1988).
[10] M. Rohlfing, P. Krüger, and J. Pollmann, Phys. Rev. B **48**, 17791 (1993).
[11] T. Kotani and M. van Schilfgaarde, Solid State Commun. **121**, 461 (2002).
[12] B. Arnaud and M. Alouani, Phys. Rev. B **62**, 4464 (2000).
[13] S. Ishii, K. Ohno, Y. Kawazoe, and S. G. Louie, Phys. Rev. B **63**, 155104 (2001).
[14] S. Ishii, K. Ohno, Y. Kawazoe, and S. G. Louie, Phys. Rev. B **65**, 245109 (2002).
[15] S. Engelsberg and J. R. Schrieffer, Phys. Rev. **131**, 993 (1963).
[16] X. Zhu, Spectrochim. Acta, Part A **61**, 2730 (2005).
[17] K. M. Song, A. K. Ray, and P. K. Khowash, J. Phys. B **27**, 1637 (1994).
[18] W. Zhao, P. L. Cao, B. X. Li, B. Song, and H. Nakamatsu, Phys. Rev. B **62**, 17138 (2000).
[19] I. Vasiliev, S. Öğüt, and J. R. Chelikowsky, Phys. Rev. B **60**, R8477 (1999).
[20] J. J. BelBruno, Heteroat. Chem. **14**, 189 (2003).
[21] L. Lou, L. Wang, L. P. Chibante, R. T. Laaksonen, and P. Nordlander, J. Chem. Phys. **94**, 8015 (1991).
[22] M. A. Al-Laham and K. Raghavachari, J. Chem. Phys. **98**, 1 (1993).
[23] M. J. Frisch, G. W. Trucks, H. B. Schlegel, G. E. Scuseria, M. A. Robb, J. R. Cheeseman, J. A. Montgomery, Jr., T. Vreven, K. N.

Kudin, J. C. Burant, J. M. Millam, S. S. Iyengar, J. Tomasi, V. Barone, B. Mennucci, M. Cossi, G. Scalmani, N. Rega, G. A. Petersson, H. Nakatsuji, M. Hada, M. Ehara, K. Toyota, R. Fukuda, J. Hasegawa, M. Ishida, T. Nakajima, Y. Honda, O. Kitao, H. Nakai, M. Klene, X. Li, J. E. Knox, H. P. Hratchian, J. B. Cross, V. Bakken, C. Adamo, J. Jaramillo, R. Gomperts, R. E. Stratmann, O. Yazyev, A. J. Austin, R. Cammi, C. Pomelli, J. W. Ochterski, P. Y. Ayala, K. Morokuma, G. A. Voth, P. Salvador, J. J. Dannenberg, V. G. Zakrzewski, S. Dapprich, A. D. Daniels, M. C. Strain, O. Farkas, D. K. Malick, A. D. Rabuck, K. Raghavachari, J. B. Foresman, J. V. Ortiz, Q. Cui, A. G. Baboul, S. Clifford, J. Cioslowski, B. B. Stefanov, G. Liu, A. Liashenko, P. Piskorz, I. Komaromi, R. L. Martin, D. J. Fox, T. Keith, M. A. Al-Laham, C. Y. Peng, A. Nanayakkara, M. Challacombe, P. M. W. Gill, B. Johnson, W. Chen, M. W. Wong, C. Gonzalez, and J. A. Pople, GAUSSIAN 03, Gaussian, Inc., Wallingford, CT, 2004.

[24] S. C. O'Brien, Y. Liu, Q. Zhang, J. R. Heath, F. K. Tittel, R. F. Curl, and R. E. Smalley, J. Chem. Phys. **84**, 4074 (1986).

[25] C. Jin, K. J. Taylor, J. Conceicao, and R. E. Smalley, Chem. Phys. Lett. **175**, 17 (1990).

[26] M. Shishkin and G. Kresse, Phys. Rev. B **74**, 035101 (2006).

[27] *Landolt-Börnstein: Numerical Data and Functional Relationships in Science and Technology*, New Series Vol. III, Pt. 22a, edited by K. H. Hekkwege, O. Madelung, M. Shulz, and H. Weiss (Springer-Verlag, New York, 1987).

[28] L. Ley, R. A. Pollak, F. R. McFeely, S. P. Kowalczyk, and D. A. Shirley, Phys. Rev. B **9**, 600 (1974).